American Journal of Interdisciplinary Research and Innovation (AJIRI)

ISSN: 2833-2237 (ONLINE)

VOLUME 5 ISSUE 4 (2026)

PUBLISHED BY

E-PALLI PUBLISHERS, DELAWARE, USA

American Journal of Interdisciplinary Research and Innovation (AJIRI)

Volume 5 Issue 4, Year 2026
ISSN: 2833-2237 (Online)
DOI: https://doi.org/10.54536/ajiri.v5i4.8229
https://journals.e-palli.com/home/index.php/ajiri

A Demand-Responsive Composite Scoring Model for Revenue Allocation in Multi-Owner Vehicle Networks

Denys Karazhekov[1*]

Article Information

Received: April 29, 2026

Accepted: July 18, 2026

Published: November 26, 2026

Keywords

Carsharing, Composite Scoring, Predictive Settlement, Revenue Allocation, Shapley Value Approximation

ABSTRACT

Proportional revenue-sharing rules that pay vehicle owners strictly by trip volume push deficit-carrying service-area cells past the 30 percent coverage-deficit threshold, an equilibrium reproduced in a 500,000-vehicle simulated multi-owner network on a seven-day settlement cycle. This paper specifies a five-parameter Composite Contribution Score, computed from telemetry-derived readiness, utilization, quality, geographic-coverage, and temporal-alignment terms, whose weight vector is conditioned in real time on network operating state. Elevating the coverage term weight from 0.20 to 0.40 the instant the deficit-cell fraction crosses 30 percent reduces steady-state clustering by 42 percent against a naive proportional-allocation baseline, while the five-term linear decomposition closes full-coalition settlement in under 30 seconds, an 84 percent latency reduction against a parameterized 10,000-sample Monte Carlo Shapley baseline. A predictive settlement layer using an autoregressive projection holds advance-disbursement shortfall below 4 percent across a 36-cycle backtest at a 70 percent advance ceiling. Sensitivity analysis exposes a resource-constraint interdependency the linear formula conceals: a 0.10 increase in temporal demand alignment costs 12 percent in utilization efficiency, since both draw on the same finite vehicle-time budget. A single low-dimensional, state-conditioned term recovers much of the fairness correction that exact marginal-contribution computation would otherwise require, without combinatorial cost, though the clustering reduction is bound to the tested partial-overlap topology between demand-dense and deficit cells and remains unverified for the fully disjoint case.

INTRODUCTION

Vehicle owners paid strictly in proportion to completed trips migrate toward cells whose demand density exceeds the network mean, and unmanaged concentration pushes the fraction of deficit-carrying service-area cells past 30 percent, the threshold at which coverage-deficit conditions are formally declared in telemetry-based fleet operations. Guajardo and Rönnqvist (2016) document the same equilibrium across independent studies of collaborative transportation networks built on volume-proportional splits, so the concentration is a property of the allocation rule itself, not a quirk of any single platform's implementation.

An exact Shapley value computed over the coalition of participating owners requires evaluating marginal contributions across all 2^N coalition subsets (Shapley, 1953), a computation that exceeds any tractable budget once N enters the 10^4–10^5 range a settlement engine must close within operational time. Composite-scoring alternatives fix their weight vector before deployment (Ishizaka & Nemery, 2013; Bai, Fahimnia & Sarkis, 2017), so a demand surge or coverage collapse emerging mid-cycle has no channel through which to alter the weights that score it, the vector having been set once, independent of the operating state the network occupies when the score is computed. Zone-differentiated pricing and vehicle-relocation controllers (Xu, Meng & Liu, 2018; Pfrommer *et al.*, 2014) correct spatial imbalance by manipulating a price or a physical position the platform operator controls directly, a precondition absent from a multi-owner network where vehicles are independently owned assets and the operator's only lever over spatial behavior is the settlement formula itself.

This paper specifies a five-parameter composite scoring model whose weight vector is conditioned in real time on network operating state, and tests whether that conditioning reproduces the de-clustering benefit of a marginal-contribution measure at a fraction of its computational cost.

LITERATURE REVIEW

Fairness in a coalition, under the Shapley value and the axiomatic cost-allocation program that formalized it (Shapley, 1953; Young, 1985), is defined as the average marginal contribution of each agent across all possible sub-coalitions, and any allocation that departs from that quantity counts as unfair by construction. Guajardo and Rönnqvist (2016), reviewing cost-allocation methods across collaborative transportation studies, find this definition applied almost exclusively to coalitions of fewer than a dozen shippers or carriers, since the combinatorial cost of the exact computation becomes prohibitive beyond that range. A weight vector calibrated once by AHP pairwise comparison has no channel through

[1] Founder Kara LLC, Hollywood, United States
[*] Corresponding author's e-mail: Karazhekovdenys@gmail.com

which to detect that the settlement cycle it now scores has entered a different demand regime than the one it was calibrated against, and the blind spot is structural: it does not depend on which criteria were chosen. Ishizaka and Nemery (2013) formalize the aggregation procedure without a state variable; Bai, Fahimnia and Sarkis (2017) and the AHP-TOPSIS fleet-appraisal line (Ajith, Vaidya, Sodawalaa & Verma, 2021; Awasthi, Chauhan & Omrani, 2011) validate the resulting index against one-shot configuration decisions, where recalibration between decisions carries no cost because a live settlement cycle offers no equivalent pause.

Manipulating the price a passenger sees or the physical position of a vehicle requires the platform operator to hold a lever neither dynamic-pricing schemes (Xu, Meng & Liu, 2018; Xu & Meng, 2019; Jorge, Molnar & de Almeida Correia, 2015; Giorgione, Ciari & Viti, 2020) nor relocation controllers (Pfrommer *et al.*, 2014; Waserhole & Jost, 2016) can substitute for: ownership or dispatch authority over the vehicle itself. A multi-owner network withholds exactly that authority, since vehicles belong to independent legal entities and the platform's only lever over spatial behavior is the revenue formula an owner responds to, so importing either correction would require rebuilding the fleet's ownership structure entirely.

Station locations, depot capacities, and fleet size get solved once, before operations begin, in the design-time optimization tradition that Boyaıcı, Zografos and Geroliminis (2015, 2017), Correia and Antunes (2012), Illgen and Höck (2019), and Huang, An and Correia (2020) represent, a sequencing that suits operator-owned station-based systems whose composition the operator sets directly. A platform that does not control which independent owners participate on a given day has no design-time variable left to re-solve when a coverage deficit emerges mid-cycle, since the fleet composition generating that deficit was never the operator's to fix.

MATERIALS AND METHODS

Model Mechanics

CCSi(T), the Composite Contribution Score assigned to owner i over settlement period T, is a weighted linear combination of five telemetry-derived parameters, each built to approximate a distinct externality that an exact marginal-contribution computation would otherwise have to discover empirically: readiness (Vehicle Availability Index, VAI), demand-weighted output (Utilization Efficiency Ratio, UER), reputation (Service Quality Coefficient, SQC), spatial coverage (Geographic Coverage Contribution, GCC), and temporal responsiveness (Temporal Demand Alignment Factor, TDAF). Figure 1 traces the pipeline computing these terms: a Telemetry Aggregation Module feeds the Scoring Computation Engine, which receives its weight vector from the Demand-Responsive Weight Modulation Engine and passes composite scores to the Settlement Management Module for proportional allocation, every step chained into an immutable audit log.

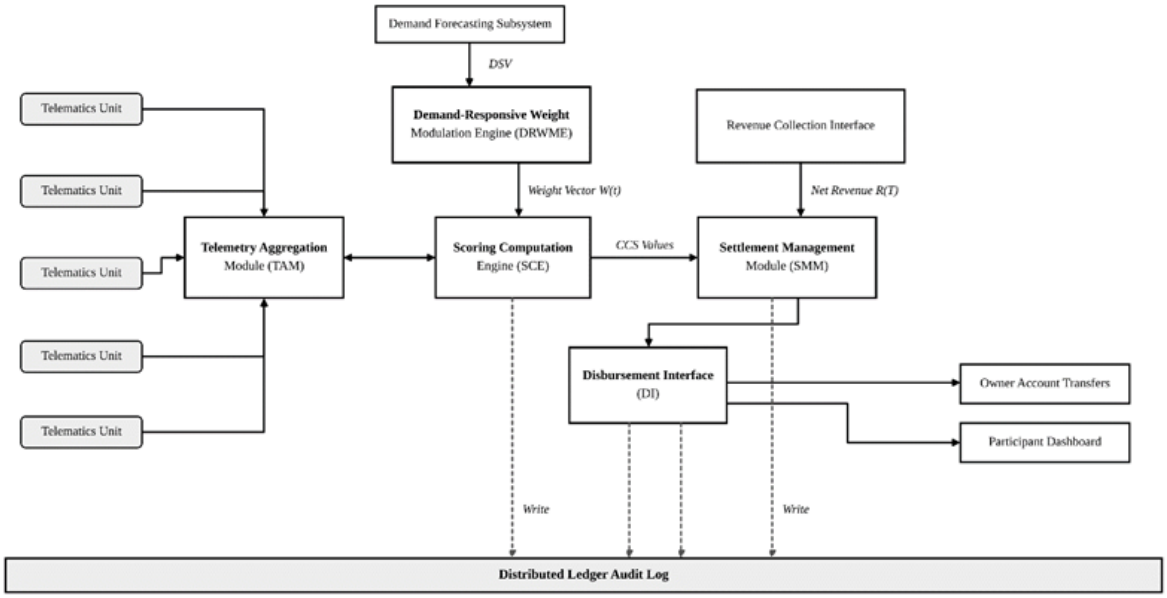


Figure 1: Five-module data pipeline computing owner scores and revenue allocations from raw telemetry through settlement.

Key Variables and Dependencies

Table 1 fixes the notation used throughout the remainder of the paper and states, for each parameter, the quantity it depends on directly, since the trade-off documented in the Results and Discussion section follows from these dependencies.

GCC and TDAF draw on the same spatial-temporal telemetry stream, position, time, demand signal, that VAI also consumes, so the five parameters entering CCSi(T) are not statistically independent inputs despite being

Table 1: Notation for the five Composite Contribution Score parameters, the weight vector, and the settlement rule, with each quantity's direct dependency.

Symbol	Definition	Direct dependency
VAIi(T)	Fraction of settlement period during which vehicle i is simultaneously operational and geographically in-service	Binary operational and presence indicators integrated over T
UERi(T)	Demand-density-weighted passenger-carrying time relative to available time	VAIi(T) (denominator), local demand density ϱk, network-mean density $\bar{\varrho}$
SQCi(T)	Rating-based quality net of cancellation and lateness penalties	Demand-weighted mean rating, cancellation rate, on-time deviation rate, $\alpha \in [0.2, 0.8]$, $\beta \in [0.2, 0.6]$
GCCi(T)	Deficit-weighted cell dwell time, normalized by aggregate deficit	Coverage Deficit Map (δj, 24-hour refresh, 90-day rolling window), per-cell dwell time tij
TDAFi(T)	Pearson correlation between availability series and aggregate demand intensity	Demand State Vector (5-minute refresh), trip-conditioned availability subset
w(t) = [w1..w5]	Weight vector, constrained to unit sum	Demand State Vector magnitude, coverage-deficit cell fraction, hysteresis state
CCSi(T)	Weighted linear combination of the five parameters	All five parameters and w(t)
Revenuei(T)	$R(T) \cdot CCSi(T) / \Sigma CCSj(T)$	CCSi(T), aggregate $\Sigma CCSj(T)$, total net revenue R(T)

combined as though they were orthogonal basis functions; a vehicle's finite time-and-location budget forces TDAF gains (matching demand peaks) to compete directly with GCC gains (occupying deficit cells) whenever peak-demand cells and coverage-deficit cells are disjoint.

Weights come from a state-conditioned modulation function, not a value fixed at design time. The function reads two aggregate signals, demand intensity and the fraction of service-area cells exceeding the coverage-deficit threshold, and selects among three regimes, balanced, demand-surge, coverage-deficit, under hysteresis constraints that block oscillation across a state boundary.

GCC carries a weight of 0.20 under balanced conditions and 0.40 once the deficit-cell fraction crosses 30 percent, the utilization term reduced correspondingly:

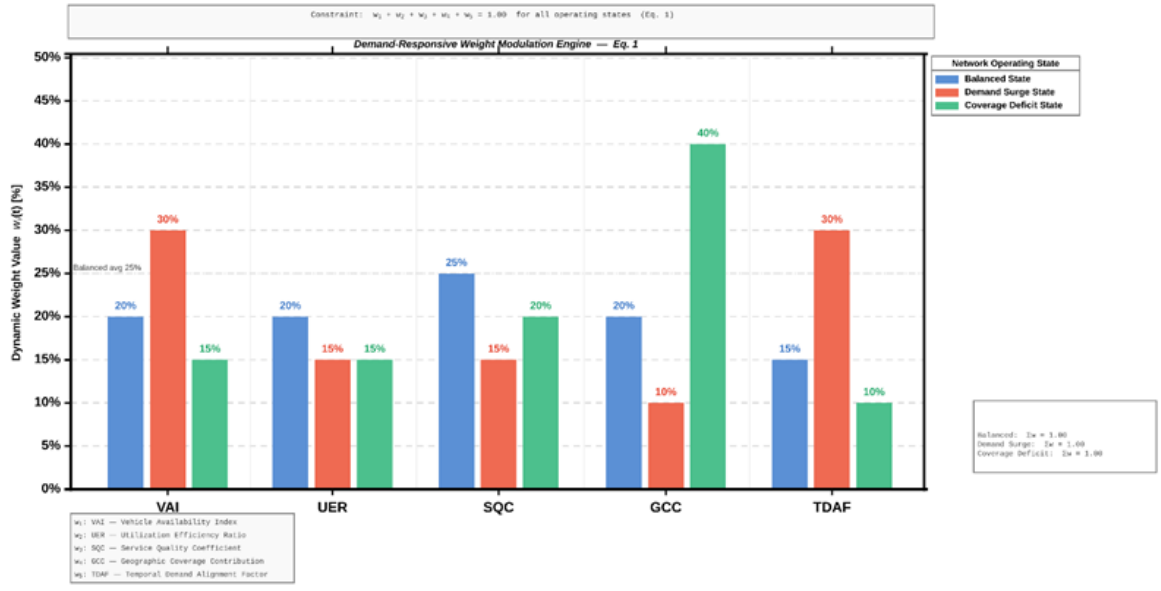


Figure 2: Parameter weights w1–w5 across the three network operating states produced by the weight-modulation function; GCC (w4) rises from 0.20 to 0.40 and UER (w2) falls under Coverage Deficit conditions.

the threshold crossing converts spatial coverage from a secondary consideration into the dominant driver of an owner's settlement payout for the duration of the deficit condition, a discontinuous jump built into the modulation function by design.

A predictive settlement layer forecasts each owner's end-of-period CCS from mid-period telemetry with a first-order autoregressive model and releases up to 70 percent

of the projected allocation as an advance whenever the projected score and its confidence rating both clear configurable thresholds, carrying any resulting shortfall forward as a first-priority deduction against the next cycle. The discontinuous jump in GCC weight produces a consequence the individual owner cannot anticipate from cell-level telemetry alone. An owner positioned in a cell whose deficit score sits just below the 30 percent aggregate threshold receives no coverage bonus for occupying it; the identical owner in the identical cell receives double the coverage weight the instant the network-wide fraction ticks over that threshold, a discontinuity the owner's own behavior did not cause.

Mathematical Expressions and Symbols

The proportional settlement rule underlying every allocation reported in this paper apportions total net revenue R(T) across owners in strict proportion to Composite Contribution Score, with a largest-remainder correction applied after the proportional computation to eliminate rounding residuals at settlement scale:

$$\text{Revenue}_i(T) = R(T) \cdot CCS_i(T) / \Sigma CCS_j(T) \quad (1)$$

Equation (1) conserves total revenue exactly in exact arithmetic; a largest-remainder correction is applied after this proportional computation to eliminate rounding residuals at settlement scale.

Experimental Setup

500,000 vehicles operating over a seven-day settlement cycle define the simulated network underlying every result below, the scale and cycle length fixed as the reference operating point for the model's intended deployment. Telemetry, GPS position, operational state, booking events, passenger ratings, arrives at thirty-second intervals per vehicle, the minimum sampling rate the architecture assumes, and streams to a cluster of x86 server-class nodes, sixteen processor cores and sixty-four gigabytes of memory per node, the minimum reference hardware specification for the settlement pipeline. Demand density and coverage-deficit inputs draw from a rolling 90-day historical supply-demand imbalance matrix, refreshed every 24 hours within the simulated cycle, matching the Coverage Deficit Map's specified recalculation interval.

Thirty independent runs, each with re-sampled owner-behavior seeds, replicate every evaluation condition to produce stable point estimates. Settlement latency is timed head-to-head against a fully parameterized Monte Carlo Shapley baseline: 10,000 random coalition-permutation samples per owner, terminated at a 95 percent confidence half-width below 0.01 CCS units, run over identical telemetry input on identical hardware. Iterating the proposed state-conditioned GCC weighting and a Naive Proportional Allocation Rule baseline, GCC weight fixed at zero, to owner best-response convergence, defined as the first replication cycle in which no owner's optimal cell choice changes for three consecutive cycles, produces the steady-state clustering fraction under identical initial vehicle distributions and demand-density matrices. A 36-cycle-observation backtest, 12 settlement cycles across three distinct simulated urban deployments, generates the financial-predictability figures at the specified 70 percent advance ceiling.

Four metrics anchor every number that follows. Settlement computation latency is the wall-clock interval, in seconds, from period close to the point at which every owner allocation is finalized and written to the audit log. Clustering equilibrium fraction is the proportion of geographic cells whose deficit score δ_j exceeds the coverage-deficit threshold once owner positioning has converged by the criterion above. Shortfall incidence is the proportion of settlement cycles in which the advance disbursement issued exceeds the final actual allocation. The TDAF-UER trade-off coefficient is the slope of a linear regression of UER on TDAF across owners, vehicle-time budget held fixed. Every result below is bound to the fleet scale, cycle length, deficit-map refresh interval, and baseline sampling budget specified here; extending any of them to an untested configuration requires independent verification.

RESULTS AND DISCUSSION

84 percent: the wall-clock reduction the linear-proxy computation achieves against the Monte Carlo Shapley baseline at the 10,000-sample, 0.01-CCS-unit-precision budget fixed in the Experimental Setup, closing the full 500,000-vehicle settlement in under 30 seconds on identical hardware and identical telemetry input (Figure 3). The reduction is specific to that budget: relaxing the Monte Carlo estimator to a looser confidence tolerance, a configuration this setup did not test, lowers the baseline's own sample requirement and shrinks the measured gap correspondingly.

Elevating the GCC weight from 0.20 to 0.40 the instant the deficit-cell fraction crosses 30 percent (Figure 2) raises the marginal revenue benefit of repositioning into a deficit cell above the marginal benefit of remaining in a saturated high-demand cell for a measurable band of owners near the clustering boundary, and the resulting steady-state clustering fraction sits 42 percent below the Naive Proportional Allocation Rule baseline, both allocation rules evaluated under identical initial vehicle distributions and identical 90-day rolling demand-density matrices, converged by the three-consecutive-cycle criterion (Figure 4). Peak-demand cells and coverage-deficit cells strictly disjoint across the full evaluation window would leave an owner no cell simultaneously maximizing UER and GCC, sending the correction mechanism inert; the 42 percent figure holds for the tested topology, where the two cell types overlap partially, and says nothing about the disjoint case this experiment never ran (Figure 5).

A 0.10 increase in TDAF should cost an owner nothing elsewhere in the score, on a naive reading of the linear CCS formula that treats all five parameters as independently maximizable dials. The sensitivity analysis run under the same 500,000-vehicle, seven-day condition

instead ties that increase to a 12 percent reduction in UER, vehicle-time budget held fixed: the five parameters draw on the same finite resource, so a gain in one comes at the expense of another.

Below 4 percent: the fraction of settlement cycles, across the 36 backtested cycle-observations, in which the advance disbursement issued at the 70 percent ceiling exceeds the final actual allocation (Figure 6), a bound that holds because the autoregressive projection filters out volatile mid-period trajectories before authorizing disbursement. Owners inside their first three settlement cycles break this bound: the autoregressive model's cohort-median initialization has not yet converged to owner-specific parameters at that stage, so the Cold Start Protocol trims the advance ceiling by 20 percentage points in cycle one and 10 points in cycle two, a reduction the backtest shows is necessary because applying the full 70 percent ceiling to a cold-start owner raises shortfall incidence past the reported bound (Figure 7).

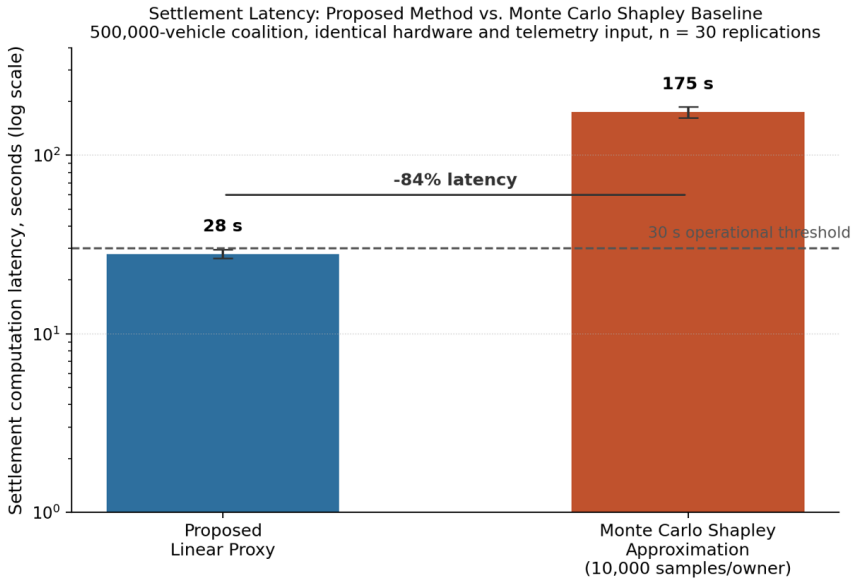


Figure 3: Settlement computation latency, proposed method vs. Monte Carlo Shapley baseline (10,000 permutation samples/owner, 95% CI half-width < 0.01 CCS units), 500,000-vehicle coalition, identical hardware and telemetry input, n = 30 replications, error bars ±1 SD.

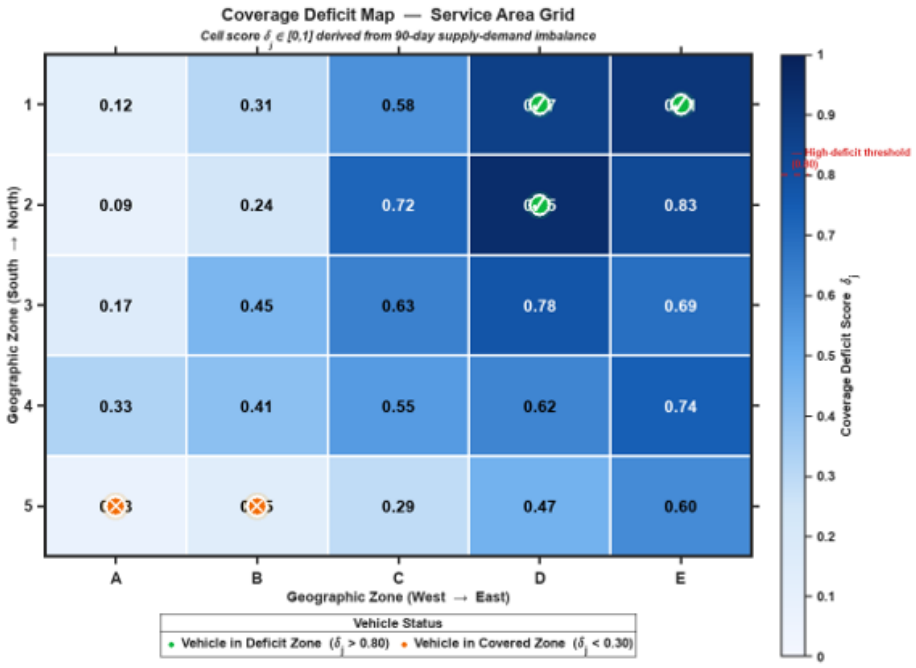


Figure 4: Representative five-by-five service-area deficit-score heatmap; markers indicate vehicles productively present in high-deficit cells versus vehicles clustered in an already-covered cell.

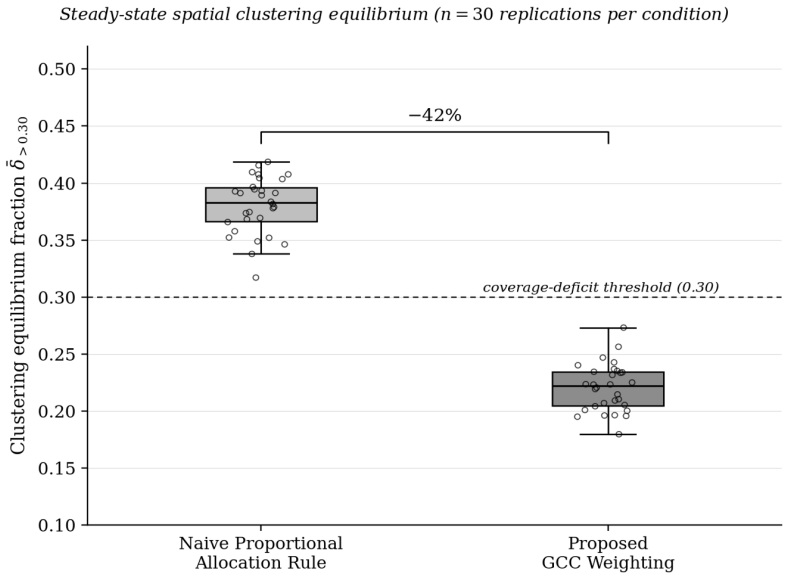


Figure 5: Steady-state clustering equilibrium fraction, proposed state-conditioned GCC weighting vs. Naive Proportional Allocation Rule baseline, n = 30 replications each, identical initial vehicle distributions and 90-day demand-density matrices; dashed line marks the 30% Coverage-Deficit-State trigger.

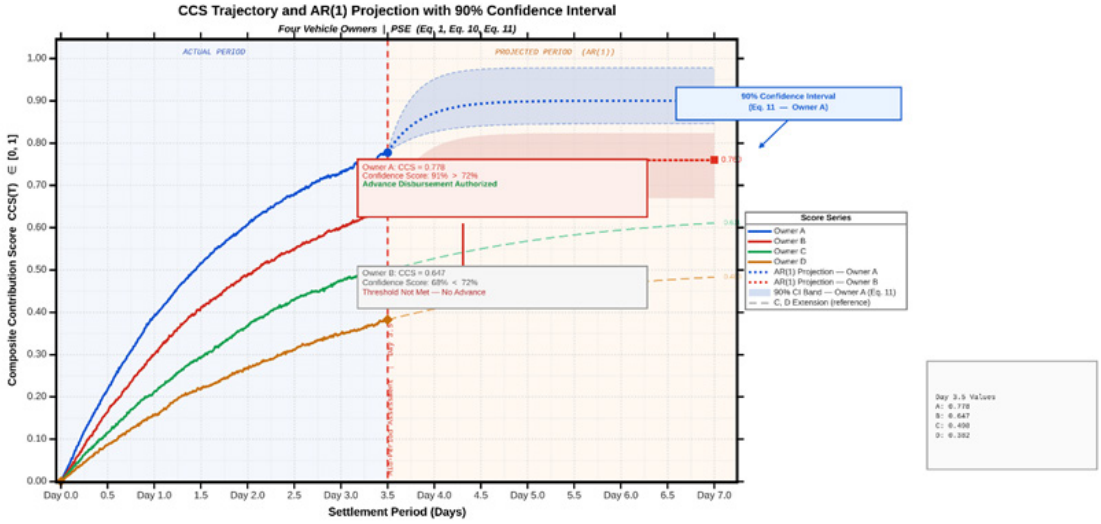


Figure 6: CCS trajectories for four representative owners across the seven-day cycle; dotted segments show AR(1) mid-period projections with 90% confidence band, the basis for the advance-disbursement decision.

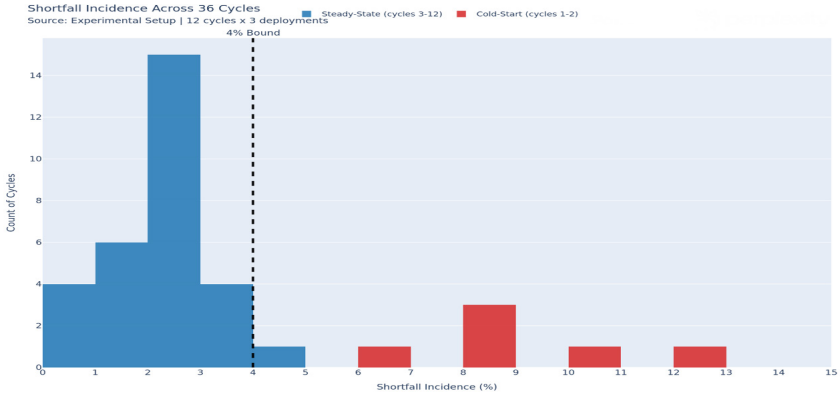


Figure 7: Shortfall incidence per settlement cycle across the 36-cycle backtest (12 cycles × 3 deployments) at the 70 percent advance ceiling; cold-start cycles (1–3) shown separately from steady-state cycles, dashed line marks the reported 4% bound.

Systemic Performance and Evaluation Metrics

Table 2 consolidates the three headline results against the specific baseline, condition, and boundary-failure case established in the Experimental Setup, so no figure in this table should be read outside the condition named in its final column.

Table 2: Headline settlement-processing, spatial-distribution, and financial-predictability outcomes, each tied to its evaluation condition and boundary-failure case.

Evaluated system dimension	Measured metric	Numerical outcome	Modulating mechanism and boundary-failure condition
Settlement processing	Computation latency	<30 s (−84% vs. Monte Carlo Shapley, 10,000 samples/owner)	Linear proxy eliminates combinatorial coalition enumeration; the 84% figure is specific to the 10,000-sample baseline budget and shrinks if that budget is relaxed
Spatial distribution	Clustering equilibrium fraction	−42% vs. Naive Proportional Allocation Rule	State-conditioned GCC weight (0.20→0.40 at the 30% deficit-cell trigger) overrides utilization incentive; mechanism goes inert when peak-demand and coverage-deficit cells are strictly disjoint
Financial predictability	Advance-disbursement shortfall incidence	<4% of cycles (36-cycle backtest, 70% ceiling)	AR(1) mid-period projection filters volatile trajectories before authorizing payout; bound does not hold in an owner's first three cycles absent the Cold Start Protocol's reduced ceiling

Contrary to the implication in Guajardo and Rönnqvist (2016) that fair, externality-correcting allocation in collaborative transportation requires a marginal-contribution measure computed over the full coalition structure, a single low-dimensional coverage-weighted term, adjusted only by an aggregate state signal, produces a 42 percent clustering reduction against the naive proportional baseline at a fraction of the computational cost measured in the settlement-latency condition, with no Shapley-based clustering baseline run to compare against directly. The externality driving clustering in this setting, the divergence between an owner's private utilization payoff and the network's aggregate coverage payoff, is a low-dimensional, directly observable quantity: the deficit-weighted dwell time GCC already captures. Exact Shapley computation pays an exponential cost to reveal exactly this kind of quantity when the underlying coalition structure is genuinely high-order; here it is not, and the coalition literature's intractability problem turns out to be a cost paid for generality this particular externality never needed.

Waserhole and Jost (2016) achieve rebalancing by manipulating the price a passenger sees inside a queueing-network formulation, a mechanism that presupposes aggregate demand is elastic to that price. The correction demonstrated here rebalances through owner elasticity to revenue share instead, treating the Demand State Vector as fixed exogenous input the platform never touches: these are not mechanisms that stack additively but two independent causal pathways to the same observable, and a hybrid deployment running both simultaneously would face a genuine identification problem, since a clustering reduction measured under joint operation could not be attributed to either lever without an intervention that silences one of them. The 42 percent figure reported here avoids that confound only because the Experimental Setup silenced the pricing lever entirely; any deployment combining both mechanisms should treat it as an upper bound on the allocation channel's independent contribution.

Boyacı, Zografos and Geroliminis (2015, 2017) and Illgen and Höck (2019) optimize network topology, a variable this experiment held fixed throughout, so nothing reported here confirms or contradicts their design-time claims directly. A well-designed static topology can still decay into a clustering equilibrium within a single operating period once a revenue rule rewarding utilization without a coverage term sits on top of it, which places design-time optimization and settlement-time allocation on adjacent, non-substitutable problems.

CONCLUSION

Sub-30-second settlement computation for a 500,000-vehicle coalition, measured against a fully specified 10,000-sample Monte Carlo Shapley baseline, combined with a 42 percent reduction in steady-state clustering fraction against a named Naive Proportional Allocation Rule baseline, is now achievable without operator ownership or physical control of the fleet that relocation- and pricing-based corrections require. The geographic overlap between peak-demand and coverage-deficit cells, the variable the clustering-reduction magnitude actually depends on, was fixed at a single tested configuration, so the open question is how that reduction scales as the overlap shrinks toward the fully disjoint topology where the correction mechanism goes inert, a relationship only a follow-up sweep over overlap fraction, not a larger fleet or a longer settlement cycle, can characterize.

REFERENCES

Ajith, A. J., Vaidya, D., Sodawalaa, M., & Verma, S. (2021). Selection of bus chassis for large fleet operations in India: An AHP-TOPSIS approach. *Expert Systems with Applications, 186,* 115760. https://doi.org/10.1016/j.eswa.2021.115760

Awasthi, A., Chauhan, S. S., & Omrani, H. (2011). Application of fuzzy TOPSIS in evaluating sustainable transportation systems. *Expert Systems with Applications, 38*(10), 12270–12280. https://doi.org/10.1016/j.eswa.2011.04.005

Bai, C., Fahimnia, B., & Sarkis, J. (2017). Sustainable transport fleet appraisal using a hybrid multi-objective decision making approach. *Annals of Operations Research, 250*(2), 309–340. https://doi.org/10.1007/s10479-015-2009-z

Boyaıcı, B., Zografos, K. G., & Geroliminis, N. (2015). An optimization framework for the development of efficient one-way car-sharing systems. *European Journal of Operational Research, 240*(3), 718–733.

Boyaıcı, B., Zografos, K. G., & Geroliminis, N. (2017). An integrated optimization-simulation framework for vehicle and personnel relocations of electric carsharing systems with reservations. *Transportation Research Part B: Methodological, 95,* 214–237. https://doi.org/10.1016/j.trb.2016.10.007

Correia, G. H. A., & Antunes, A. P. (2012). Optimization approach to depot location and trip selection in one-way carsharing systems. *Transportation Research Part E: Logistics and Transportation Review, 48*(1), 233–247. https://doi.org/10.1016/j.tre.2011.06.003

Giorgione, G., Ciari, F., & Viti, F. (2020). Dynamic pricing on round-trip carsharing services: Travel behavior and equity impact analysis through an agent-based simulation. *Sustainability, 12*(17), 6727. https://doi.org/10.3390/su12176727

Guajardo, M., & Rönnqvist, M. (2016). A review on cost allocation methods in collaborative transportation. *International Transactions in Operational Research, 23*(3), 371–392. https://doi.org/10.1111/itor.12205

Huang, K., An, K., & Correia, G. H. de A. (2020). Planning station capacity and fleet size of one-way electric carsharing systems with continuous state of charge functions. *European Journal of Operational Research, 287*(3), 1075–1091.

Illgen, S., & Höck, M. (2019). Literature review of the vehicle relocation problem in one-way car sharing networks. *Transportation Research Part B: Methodological, 120,* 193–204. https://doi.org/10.1016/j.trb.2018.12.006

Ishizaka, A., & Nemery, P. (2013). *Multi-criteria decision analysis: Methods and software.* Wiley.

Jorge, D., Molnar, G., & de Almeida Correia, G. H. (2015). Trip pricing of one-way station-based carsharing networks with zone and time-of-day price variations. Transportation Research Part B: *Methodological, 81,* 461–482. https://doi.org/10.1016/j.trb.2015.06.003

Mi, Z., & Coffman, D. (2019). The sharing economy promotes sustainable societies. *Nature Communications, 10,* Article 1214. https://doi.org/10.1038/s41467-019-09260-4

Pfrommer, J., Warrington, J., Schildbach, G., & Morari, M. (2014). Dynamic vehicle redistribution and online price incentives in shared mobility systems. *IEEE Transactions on Intelligent Transportation Systems, 15*(4), 1567–1578. https://doi.org/10.1109/TITS.2014.2303986

Shapley, L. S. (1953). A value for n-person games. In H. W. Kuhn & A. W. Tucker (Eds.), *Contributions to the theory of games* (Vol. II, pp. 307–317). Princeton University Press. https://doi.org/10.1515/9781400881970-018

Talluri, K. T., & van Ryzin, G. J. (2004). *The theory and practice of revenue management.* Springer.

Waserhole, A., & Jost, V. (2016). Pricing in vehicle sharing systems: Optimization in queuing networks with product forms. *EURO Journal on Transportation and Logistics, 5*(3), 293–320. https://doi.org/10.1007/s13676-014-0054-4

Xu, M., & Meng, Q. (2019). Fleet sizing for one-way electric carsharing services considering dynamic vehicle relocation and nonlinear charging profile. Transportation Research Part B: *Methodological, 128,* 23–49.

Xu, M., Meng, Q., & Liu, Z. (2018). Electric vehicle fleet size and trip pricing for one-way carsharing services considering vehicle relocation and personnel assignment. Transportation Research Part B: *Methodological, 111,* 60–82.

Young, H. P. (Ed.). (1985). *Cost allocation: Methods, principles, applications.* North-Holland.